Free Radical Research, May 2010; 44(5): 563–576

informa
healthcare

Oxidative stress in the denervated muscle

PROVVIDENZA M. ABRUZZO[1], SIMONA DI TULLIO[1], COSETTA MARCHIONNI[1], SILVIA BELIA[2], GIORGIO FANÓ[2,3], SANDRA ZAMPIERI[4,5], UGO CARRARO[4,5], HELMUT KERN[6,7], GIANLUCA SGARBI[8], GIORGIO LENAZ[8] & MARINA MARINI[1,3]

[1]*Department of Histology, Embryology, and Applied Biology, University of Bologna, Italy,* [2]*Department of Basic and Applied Medical Sciences, University G. d'Annunzio, Chieti, Italy,* [3]*Interuniversity Institute of Myology, Italy,* [4]*Laboratory of Translational Myology, Interdepartmental Research Institute of Myology, Italy,* [5]*Italian C.N.R. Institute of Neuroscience, c/o Department of Biomedical Sciences, University of Padua, Italy,* [6]*Department of Physical Medicine and Rehabilitation, Wilhelminenspital, Wien, Austria,* [7]*Ludwig Boltzmann Institute of Electrical Stimulation and Physical Rehabilitation, Wien, Austria, and* [8]*Department of Biochemistry, University of Bologna, Italy*

(Received date: 23 October 2009; In revised form date: 15 January 2010)

Abstract

Following experimental hind limb denervation in rats, this study demonstrates that oxidative stress occurs and advances an hypothesis about its origin. In fact: (i) ROS are formed; (ii) membrane lipids are oxidized; (iii) oxidized ion channels and pumps may lead to increased $[Ca^{2+}]_i$; all the above mentioned events increase with denervation time. In the denervated muscle, (iv) mRNA abundance of cytoprotective and anti-oxidant proteins (Hsp70, Hsp27, Sod1, Catalase, Gpx1, Gpx4, Gstm1), as well as (v) SOD1 enzymatic activity and HSP70i protein increase; (vi) an unbalance in mitochondrial OXPHOS enzymes occurs, presumably leading to excess mitochondrial ROS production; (vii) increased cPLA2α expression (mRNA) and activation (increased $[Ca^{2+}]_i$) may lead to increased hydroperoxides release. Since anti-oxidant defences appear inadequate to counterbalance increased ROS production with increased denervation time, an anti-oxidant therapeutic strategy seems to be advisable in the many medical conditions where the nerve-muscle connection is impaired.

Keywords: *Skeletal muscle, denervation, oxidative stress, mitochondria*

Introduction

Muscle atrophy may result from a wide range of conditions including cancer, neurodegenerative diseases, traumas and ageing [1–4].

Several evidences suggest that Reactive Oxygen Species (ROS) and mitochondrial dysfunction play an important role in muscle atrophy. ROS production is increased in muscle mitochondria and is correlated with muscle atrophy during ageing [5]. $Sod1^{-/-}$ mice showed an increase in oxidative damage levels and an age-dependent loss of muscle mass [5,6]. Furthermore, both transgenic $Sod1^{G93A}$ (expressing a mutant form of Sod1 gene) and Sod1 H46RH48Q (a metal-deficient mutant) mouse models of ALS showed an increase in oxidative stress and muscle atrophy [6,7].

ROS cause the oxidation of membrane phospholipids, proteins and DNA [8]; their toxic effects can be prevented by scavenging enzymes such as superoxide dismutase (SOD1 and SOD2), Glutathione Peroxidase 1 (GPX1) or Glutathione S-Transferase MU 1 (GSTM1), as well as by other non-enzymatic anti-oxidants. However, when the production of ROS exceeds the capacity of anti-oxidant defences, oxidative stress might have a harmful effect on the functional and structural integrity of biological tissue.

Muscle atrophy was associated to alteration in innervation of skeletal muscle. Innervation is an important trophic and regulatory factor controlling the structural and functional integrity of skeletal

Correspondence: Professor Marina Marini, Department of Histology, Embryology, and Applied Biology, University of Bologna, Via Belmeloro, 8, 40126 Bologna, Italy. Tel: (+39)0512094116. Fax: (+39)0512094110. Email: marina.marini@unibo.it

ISSN 1071-5762 print/ISSN 1029-2470 online © 2010 Informa UK Ltd. (Informa Healthcare, Taylor & Francis AS)
DOI: 10.3109/10715761003692487

muscles. The loss of innervation (denervation), following traumas, genetic and degenerative diseases or ageing results in a decline of muscle mass and force and in a rapid loss of its functional capacity [9–11].

It was demonstrated that an increase in ROS production takes place in muscle mitochondria isolated from hind limb muscle following surgical sciatic nerve transection [6]. In the skeletal muscle, oxidative damages might affect the Ryanodine-type Ca^{2+} release channel (RyR1) which, together with other Ca^{2+} handling systems, controls the intracellular Ca^{2+} concentration and consequently the skeletal muscle contractile function. The activity of RyR1 channel is dramatically affected by redox modifications of critical thiols and an extensive oxidation leads to an irreversible inactivation of RyR1 channels [12]. Also other ionic channels and pumps of the sarcolemma and of SR may be affected by oxidative stress, thus decreasing their ability to handle the ionic changes that regulate muscle contractility. It should also be mentioned that increased cellular ROS may also play a role in muscle atrophy through signalling, by modulating NF-κB [13] or TNF-α [14] inflammatory pathways, which in turn leads to the upregulation of Atrogin-1/MAFbx and the 26S proteasome system [15].

To study the effects of denervation, which occur in several years in humans, we used a rat model in which these events take place in a short space of time (weeks or months). In this paper we explore more in detail the molecular mechanisms of oxidative stress during denervation. Rat Tibialis Anterior skeletal muscle, following surgical sciatic nerve transection, was isolated after 15 days or 3 months from surgery. ROS production, lipid peroxidation, ionic channel and pump activities were assessed in intact and denervated muscles. Anti-oxidant capacity was evaluated studying the differential expression of anti-oxidant and stress-related genes and the SOD1 and SOD2 activity. The expression of different enzymes involved in oxidative phosphorylation was evaluated on the basis of the fact that the mitochondrial electron transport chain is considered the most relevant site for ROS formation. The present paper is aimed at a better understanding of the molecular pathway of denervation, in order to improve the current knowledge and the effectiveness of therapeutic interventions.

Materials and methods

Animals and muscle denervation

Two month old female Sprague-Dawley rats were used for all denervation experiments. The animals were maintained under specific pathogen-free conditions, housed in individual cages and fed *ad libitum*. The sciatic nerve of hind limbs was cut at the level of trochanter, ~1 cm nerve was removed and the peripheral stump was tied. The proximal stump was also tied and sutured into a superficial muscle to reduce chance of reinnervation and obtain permanent denervation of the hind legs. The animals rapidly recovered and showed moderate impairment of locomotion. Fifteen days or 3 months post-denervation rats were killed and the Tibialis Anterior muscles (TA) of both limbs were aseptically isolated and immediately frozen in liquid nitrogen. Muscles were then stored at –80°C until use. Each experimental group was made up of four rats, which were bilaterally denervated; the control group was made up of four Sprague-Dawley female rats which did not undergo surgery. TA from left limbs was used for the study of lipid peroxidation and ion channel activities, whereas TA from right limbs was used for the other evaluations. All experiments were carried out with the approval of Padua University Ethic Committee.

ROS production, lipid peroxidation and ion channel activities

ROS production. ROS production was determined using a fluorescent based-method as previously described by Degli Esposti [16]. The method exploits the oxidation by ROS of the fluorogenic probe dichlorodihydrofluorescein (H_2DCF, Sigma-Aldrich, St. Louis, MO), to a fluorescent product (DCF), which can be measured fluorimetrically. H_2DCF is preferentially oxidized by H_2O_2, but also by organic hydroperoxides, such as lipid hydroperoxides [17].

In brief, frozen tissue was homogenized in a lysis buffer containing 10 mM TRIS-HCl, 50 mM KCl, 1 mM EDTA and 3% Protease Inhibitor Cocktail (Sigma-Aldrich, St. Louis, MO). Protein lysates (0.5 mg/μl) were added to a reaction mixture containing 1 μM H_2DCF in phosphate-buffer saline (PBS) pH 7.4. Fluorescence was monitored for at least 45 min using a 96-well plate reader (Victor^2 Multilabel Counter, Perkin-Elmer, Waltham, MA); excitation and emission wavelengths were 485 nm and 520 nm, respectively. Data were expressed as mean differences between $T_{45\ min}$ and $T_{0\ min}$ Fluorescence Units (FU) per milligram of protein ± SD.

Purification of the cell membranes. Sarcoplasmic reticulum (SR) membranes were prepared by the method of Rock et al. [18], while the sarcolemmal fraction was purified from TA muscles as indicated by Renganathan et al. [19]. The preparations were used to evaluate the amount of lipid peroxidation products and the activities of ion channels.

Lipid peroxidation. The membrane damage induced by lipid peroxidation activity was determined by the method of TBARS as previously described [20].

RYR-1 Ca^{2+}-channels. The activity of SR RYR-1 Ca^{2+}-channels was evaluated in a free-cell condition using a specific binding methodology. SR vesicles were washed in binding buffer and centrifuged at 100 000 × g for 90 min and then resuspended in binding buffer at a final concentration of 1 mg/ml. Aliquots (65 mg) of protein were incubated at 25°C in a final 250 ml volume of binding buffer containing 10 nM [^{3}H]ryanodine for 120 min, then filtered with Whatman GF/C filters (Whatman International Ltd, Banbury, UK) and washed with six volumes of ice-cold 10 mM HEPES (pH 7.4) with 200 mM KCl. The amount of bound [^{3}H]ryanodine ([9,21-^{3}H] Ryanodine (61.5 Ci/mmol), Du Pont-New England Nuclear, Boston, NE) was determined by liquid scintillation [21].

SR Ca^{2+}-ATPase. This activity was measured on 50 µg of protein in a final volume of 1 ml of incubation medium containing 2.5 mM ATP, plus 10 µM $CaCl_2$ according to a previously reported method [21].

Sarcolemmal dihydropyridine receptor/L-type Ca^{2+}-channel (DHPR). This activity was determined as previously reported [21], using the radioligand [^{3}H] PN200-110 ([methyZ-^{3}H]PN200-1 (80 Ci/mmol), Amersham Corp., Louisville, CO). Protein (100 mg) was incubated in a final volume of 250 ml binding buffer in the presence of 1 nM [^{3}H]PN200-110 for 1 h at room temperature, following which samples were filtered with Whatman GF/C filters and washed with six volumes of ice-cold washing buffer. Radioactivity was determined by liquid scintillation counting. Non-specific [^{3}H]PN200-110 binding was assessed in the presence of 10 mM unlabelled nifedipin (Sigma-Aldrich, St. Louis, MO).

Sarcolemmal Na^+/K^+-ATPase. This activity was measured as previously reported [21]. Protein (25 mg) was incubated in 1 ml medium (134 mM NaCl, 21 mM KCl, 1 mM EGTA, 25 mM HEPES, 2.5 mM ATP, pH 7.5) in the presence or absence of 1 mM ouabain (Sigma-Aldrich, St. Louis, MO). After 10 min incubation at 37°C, the reaction was stopped by the addition of 12.5% TCA (1 ml) and the precipitate removed by centrifugation at 5000 × g for 10 min. Released orthophosphate was determined on 1 ml clear supernatant.

Sarcolemmal Ca^{2+}/Mg^{2+}-ATPase. This activity was measured as previously reported [21] on 30 mg aliquots of protein in a final volume of 1 ml medium containing 5 mM ATP and 10 mM $CaCl_2$.

RNA preparation and real-time quantitative PCR

Frozen TA muscle tissues were reduced to powder using a sterilized ceramic mortar and pestle. Total RNA was isolated homogenizing muscle powder in TRIZOL® Reagent (Invitrogen, Carlsbad, CA) according to manufacturer's instructions [22].

RNA quality was assessed by evaluation of 28S and 18S band sharpness after denaturing electrophoresis and its concentration was measured by a spectrophotometer (Ultrospec 3000, Pharmacia Biotech, Cambridge, UK). Genomic DNA contaminations were removed by digestion with RNase-free Deoxyribonuclease I (DNase I) (Amplification Grade DNase I, Sigma-Aldrich, St. Louis, MO) and its absence was assessed by PCR analysis with specific primers for Keratin 19 promoter (left: tggctcactctctcctccat, right: cataaggcatttggcacctt) [23,24].

Real-time quantitative PCR was carried out as previously described [23,24]. Equal amounts of total RNA were reverse transcribed using the Omniscript Reverse Transcription Kit (Qiagen GmbH, Hilden, Germany) following the manufacturer's instructions.

Real-time PCR was performed in a ABI PRISM 5700 real-time thermal cycler (Applied Biosystems, Warrington, UK) using the SYBR® Green PCR Master Mix (Applied Biosystems, Warrington, UK) according to the manufacturer's instructions.

Primers were designed at the 3′ end using two free softwares, PRIMER 3 and AMPLIFY, and were purchased from PROLIGO (Proligo, France SAS). To confirm primer specificity, PCR products were subjected to both melting curve analysis and to agarose gel electrophoresis. The housekeeping gene *Muscle Creatine Kinase* (Ckm) was used for normalization, since its expression does not change after denervation [25,26]. The primer sequences used in these experiments are summarized in Table I.

Real-time PCR was initially run with Ckm primers alone in order to adjust sample concentration to the same amount of Ckm cDNA. Subsequently, the differential expression of the other genes was evaluated using a relative quantification method based on threshold cycle (Ct value) [27]. At least two independent evaluations, each in quadruplicate, were carried out.

SOD activity assay

SOD activity was determined by a competitive colourimetric inhibition assay [28,29] as previously described [23]. Xanthine-Xanthine Oxidase (Sigma-Aldrich, St. Louis, MO)-generated $O_2^{\cdot-}$ was used to reduce WST-1 (water soluble tetrazolium salt 2-(4-iodophenyl)-3-(4-nitrophenyl)-5-(2,4-disulphophenyl)-2H-tetrazolium, monosodium salt, Dojindo Laboratories Co., Kumamoto, Japan) to a water-soluble formazan dye. SOD activity reduced the superoxide ion concentration and thereby inhibited the rate of WST-1 formazan formation.

Frozen tissues were reduced to powder using a sterilized ceramic mortar and pestle. The powder was homogenized in a lysis buffer containing 10 mM TRIS, 1 mM EDTA, 0.1% TRITON X-100 and 3% Protease Inhibitor Cocktail (Sigma-Aldrich, St. Louis, MO).

Table I. Primer sequence and amplicon length of the genes studied with real-time PCR. The Ckm gene was chosen for normalization purposes.

Unigene accession no	Gene	Left primer	Right primer	Amplicon length (bp)
Rn.3001	Catalase	ATTCAGAGGAAAGCGGTCAA	CCAGCGATGATTACTGGTGA	249
Rn.66581	Citrate Synthase	AGGCTAAAGGTGGGGAAGAG	CACTGTTGAGGGCTGTGATG	215
NC_001665	CoxI/mt-Co1	TTGGTGTCCTCTTCCCTGTC	TACTGGGGATGGGTAGCAAG	186
Rn.10162	cPla2α	AGCCCTCCATTCAAGGAACT	CTTCAATCCTTCCCGATCAA	105
Rn.11323	Gpx1	GTTCCAGTGCGCAGATACAG	AACACCGTCATGGAAAAACC	163
Rn.3647	Gpx4	CCGGCTACAATGTCAGGTTT	ACGCAGCCGTTCTTATCAAT	166
Rn.202944	Gstm1	TCATTCTCCCCACTTTCTTTCA	GAACAGGCTGGCACTGAGAC	153
Rn.3841	Hsp27/Hspb1	ACGAAGAAAGGCAGGATGAA	CGCTGATTGTGTGACTGCTT	161
Rn.1950	Hsp70/Hspa1a	TCTAACACGCTGGCTGAGAA	CACCCTGAGAGCCAGAAAAG	205
Rn.220465	Nox1	TCCCTTTGCTTCCTTCTTGA	CCAGCCAGTGAGGAAGAGTC	208
Rn.19172	Pgc1alpha/ Ppargc1a	ATGAGAAGCGGGAGTCTGAA	GCAGATTTACGGTGCATTCC	171
Rn.6059	Sod1	CATTCCATCATTGGCCGTA	GGCTTCCAGCATTTCCAGT	100
Rn.10488	Sod2	GCTGTGCACTGTTGAAATGC	CTGACCACAGCCTTTTTGGT	164
Rn.202951	Xdh	GTTTGTCCGCAACTGGATTT	ATCAATGGCAGGATTCAAGC	195
Rn.10756	Ckm	GGCGTAAAGCTTATGGTGGA	CAAAGTCGGTTGGTTGGACT	156

The homogenate was clarified by centrifugation at 10 000 × g for 10 min at 4°C to remove cell debris. The supernatant was stored at –80°C until use.

To determine total SOD activity, the supernatant was added to the reaction mixture in a 96-well microplate that was stirred and incubated for 20 min at 37°C.

The reaction mixture contained 500 μM WST-1, 50 μM xanthine and Xanthine Oxidase (29 mU/mL) in 50 mM CHES (2-N-[Cyclohexylamino] ethanesulphonic acid, Sigma-Aldrich, St. Louis, MO), pH 8.0.

Reduction of WST-1 was measured at 450 nm using a 96-well plate reader (Victor2 Multilabel Counter, Perkin-Elmer, Waltham, MA). SOD from bovine erythrocytes (Sigma-Aldrich, St. Louis, MO) was used as a standard for estimation of SOD activity.

To measure mitochondrial Mn-SOD (SOD2), KCN was added to tissue lysates at the final concentration of 1 mM to inhibit cytosolic Cu,Zn-SOD (SOD1). The amount of protein that inhibits the WST-1 reduction to 50% of maximum is defined as 1U of SOD activity. SOD1 was calculated as the difference between total and SOD2 activities. Enzymatic activity was expressed in units per milligram of protein.

Citrate synthase activity assay

The citrate synthase activity was assayed essentially by incubating lysate samples with 0.02% Triton X-100 and monitoring the reaction by measuring the rate of free coenzyme A release spectrophotometrically [30]. Enzymatic activity was expressed as nmol/min/mg of protein. Two independent experiments were carried out.

Western blotting

Frozen tissues were lysed in lysis buffer containing 10 mM TRIS-HCl, 50 mM KCl, 1 mM EDTA, 1% NONIDET P-40 and 3% Protease Inhibitor Cocktail (Sigma-Aldrich, St. Louis, MO). Lysates were clarified by centrifugation at 10 000 × g for 10 min and the supernatants were assayed for protein concentration by the method of Lowry et al. [31] in the presence of 0.3% (w/v) sodium deoxycholate. Equal amounts of protein (25 μg) were subjected to SDS-PAGE (either 12% or 12–20% gradient gel) and then electroblotted to nitrocellulose membranes. Membranes were saturated in blocking solution (2% dry milk, 0.05% Tween 20 in PBS solution) and the immunodetection was carried out, as described in Genova et al. [32] using a cocktail of primary mouse monoclonal antibodies (1:1000 dilution) specific for single sub-units of each OXPHOS complex (MitoSciences Inc., Eugene, OR). Cyclophilin D (MitoSciences Inc., Eugene, OR) (18 kDa) immunostaining was used as an index of the total amount of mitochondrial proteins.

Mouse anti-rat HSP70i primary antibody was purchased from Stressgen (Victoria, BC, Canada) and used at 1:1000 dilution. Mouse anti-rat beta-Actin primary antibody was purchased from Sigma-Aldrich (St. Louis, MO) and used at 1:1000 dilution. HRP-conjugated goat anti-mouse IgG secondary antibody was purchased from Pierce (Thermo Fisher Scientific, Rockford, IL) and used at 1:10 000 dilution.

PageRuler™ Plus Prestained Protein Ladder was purchased from Fermentas (Burlington, Ontario); Precision Plus™ Low Molecular Weight Prestained Protein Ladder was purchased by BioRad (Hercules, CA).

The signal was visualized using a chemiluminescent technique based on the ECL™Western Blotting Detection Reagent Kit (Amersham Biosciences, Piscataway, NJ), followed by exposure of the membranes to Fluor-S Max MultiImager system (BioRad, Hercules, CA); which also allowed the performance of the densitometric analysis. Results were expressed as HSP70i-to-beta-Actin ratio.

Statistical analysis

All data were expressed as mean ± SD. Analysis of variance (ANOVA) test was performed and the significance level was set to $p \leq 0.05$.

Results and discussion

Ros production increases following denervation

To test whether denervation induced an increase in ROS production, we measured ROS generation by DCF probe in homogenates from rat Tibialis Anterior skeletal muscle in control intact muscle and 15-days or 3-months after denervation. It should be stressed that all methods for ROS detection may lend to some artifacts; in particular, the homogenization of skeletal muscle may release iron from the intracellular stores, which then participates in Fenton reactions; the addition of EDTA to the homogenization buffer is expected to prevent the iron-mediated ROS generation. Moreover, DCF may undergo spontaneous oxidation. In the attempt to minimize this drawback, the samples were evaluated three times in different days, always with freshly prepared DCF solutions.

As shown in Figure 1A, the rate of ROS production was highly enhanced in denervated muscle homogenates and increased as a function of denervation time. Figure 1B compares the amount of ROS produced at the end of the 45 min recording. Fifteen days post-denervation, ROS production was 7.9-fold ($p < 0.01$) higher in the denervated limb compared with control. In 3-month denervated muscle, the increase in ROS generation was even greater, i.e. 64.1-fold ($p < 0.01$) higher than control and 7.6-fold ($p < 0.01$) higher than 15-day denervated muscle. The difference among the groups was so clear-cut that we are confident that it was not artifactual, notwithstanding the potential faults of the methodology.

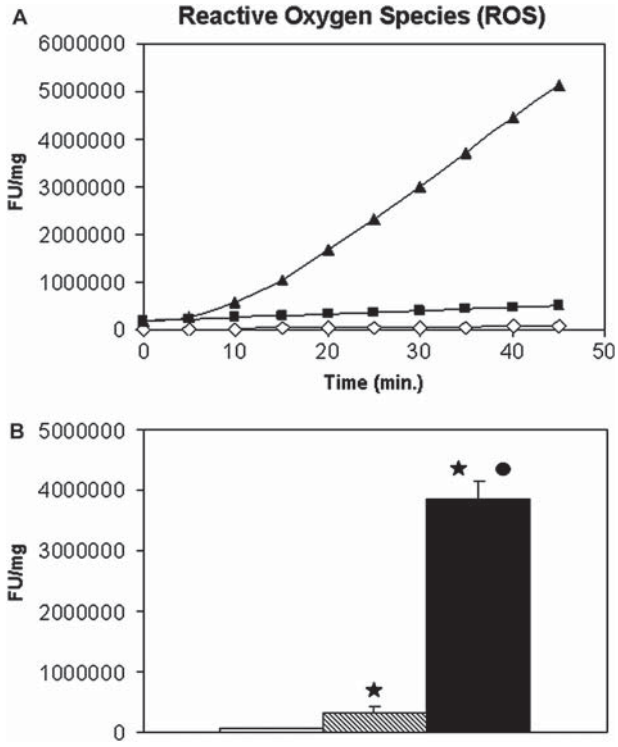

Figure 1. Reactive oxygen species (ROS). ROS oxidized the fluorogenic probe dichlorodihydrofluorescein to DCF, which was measured fluorimetrically. (A) Development of ROS production with time (0–45 min): a representative run of normal control (white diamond), 15-day denervated (black square) and 3-month denervated (black triangle) rat Tibialis Anterior homogenates. Data are expressed as Fluorescence Units (FU) per milligram of protein. (B) ROS production in normal control (open bars) or in 15-day denervated (hatched bars) or in 3-month denervated (black bars) rat Tibialis Anterior homogenates. For each sample, differences between $T_{45\ min}$ and $T_{0\ min}$ Fluorescence Units (FU) per milligram of protein were averaged and expressed as mean ± SD. Two independent evaluations per sample, each in triplicate, were carried out. ANOVA test analysis was performed. Black star: $p \leq 0.01$ vs control; black ball: $p \leq 0.01$ vs 15-day denervated.

Oxidation affects muscle cell membranes

The oxidative damage of muscle membranes was evaluated in both Sarcoplasmic Reticulum (SR) and Sarcolemma by the method of TBARS. When applied to purified membrane fractions, the interference with soluble TBARS is minimized, thus making the method fully relievable. Denervated fibres exhibited a significant increase in lipid peroxidation products (see Figure 2) with respect to controls, thus suggesting that the presence of excess ROS may possibly affect the integrity of cell membranes.

Ionic channel and pumps are damaged

Membrane ion channels are very sensitive to oxidative damage, which impairs their ability to control ion release; in muscle fibres, such impairment affects the functionality of the EC coupling apparatus. Figure 3 shows that all the examined ionic channels and pumps displayed a decreased activity in 15-day and 3-month denervated muscles when compared to intact controls.

The [^{3}H]Ryanodine binding to the SR Ca^{2+}-release channels is a marker of the ability of SR terminal cisternae to release Ca^{2+}; in 15-day and 3-month denervated muscles [^{3}H]ryanodine binding was decreased to 45.0% and 32.5%, respectively, of control values (see Figure 3A), thereby indicating a decreased capacity of Ca^{2+}channels to be maintained in the open state.

The SR Ca^{2+} pump is an indicator of the ability of SR membranes to uptake Ca^{2+}; Figure 3B shows that its ability to be phosphorylated was decreased in denervated muscles; in fact, its activity decreased to 61.0% and 54.4% of control values, in 15-day and 3-month denervated muscles, respectively.

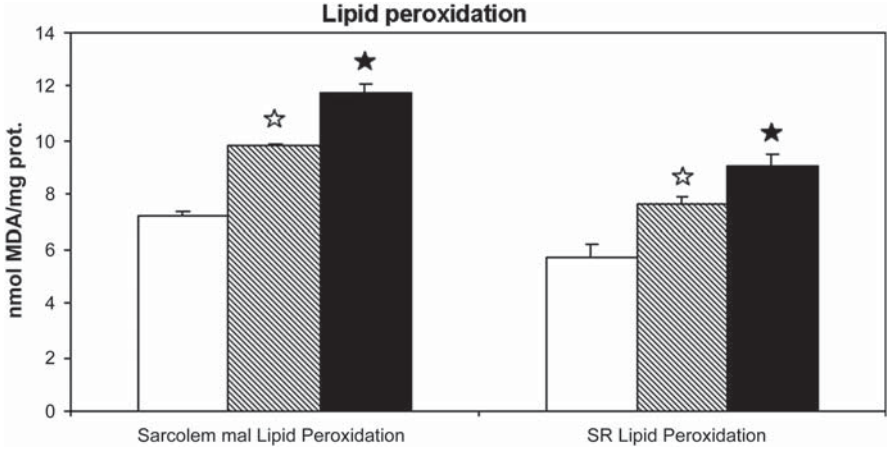

Figure 2. Lipid peroxidation in normal control (open bars) or in 15-day denervated (hatched bars) or in 3-month denervated (black bars) rat Tibialis Anterior, evaluated in Sarcolemmal (left) and in Sarcoplasmic Reticulum (SR) (right) membranes. Membranes were purified and lipid peroxidation activity was determined by the method of TBARS. Data are expressed as mean ± SD. ANOVA test analysis was performed. White star: $0.05 \geq p \leq 0.01$ vs control; black star: $p \leq 0.01$ vs control.

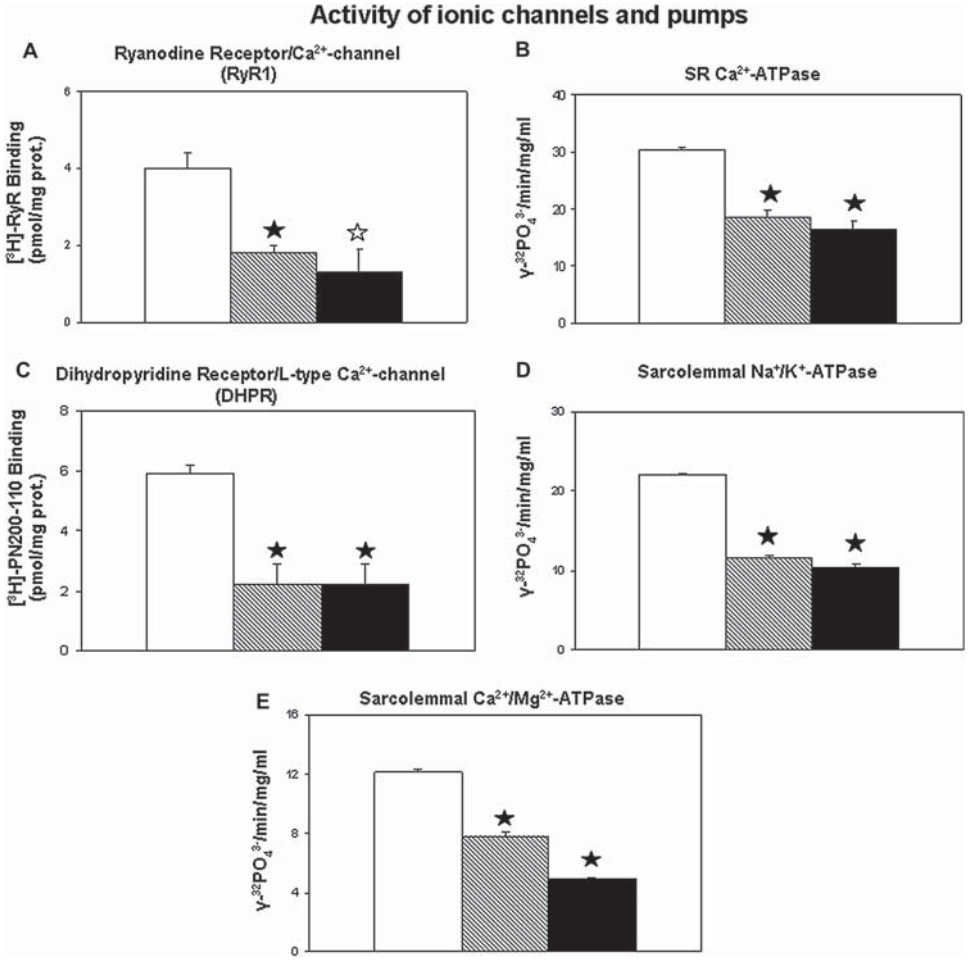

Figure 3. Activity of ionic channels and pumps in normal control (open bars) or in 15-day denervated (hatched bars) or in 3-month denervated (black bars) rat Tibialis Anterior. The RyR1 Sarcoplasmic Reticulum (SR) Ca^{2+}-channel activity was evaluated by [^{3}H] Ryanodine binding to the SR. The SR Ca^{2+}-ATPase and the plasmalemma Na^+/K^+- and Ca^{2+}/Mg^{2+}-ATPases were evaluated by measuring the amount of released γ-$^{32}PO_4^{3-}$ in controlled conditions. The activity of the Dydropyridine Receptor (DHPR)/L-type Ca^{2+}-channel of the T tubule was evaluated by the specific binding of the radioligand [^{3}H]PN200-110. Data are expressed as mean ± SD. ANOVA test analysis was performed. White star: $0.05 \geq p \leq 0.01$ vs control; black star: $p \leq 0.01$ vs control.

The amount of Dihydropyridine receptors (DHPRs) in T-tubules membranes is evaluated by measuring the [3H]PN200-110 binding to L-type Ca^{2+}-channels. Figure 3C shows a marked decrease in [3H]PN200-110 binding (37.3% of control values, in both 15-day and 3-month denervated muscles), which suggests that denervation induced a down-regulation of the excitation-contraction coupling apparatus at the sarcolemmal site.

The activities of two ionic pumps localized in the sarcolemma were examined as well. Na^+/K^+-ATPase specific activity is a marker of the physiological capacity of plasmalemma that correlates with both membrane excitability and muscle contractility. The activity of this enzyme (see Figure 3D) was found to be decreased in 15-day and 3-month denervated muscles (52.5% and 47.0% of control values, respectively).

The activity of the Ca^{2+}/Mg^{2+}-ATPase is an index of the ability of the cell to re-equilibrate cytoplasmic Calcium concentration. The activity of such ATPase in 15-day and 3-month denervated muscles was found to be 66.7% and 41.7% of control values, respectively (see Figure 3E).

It is possible that all the above reported alterations result from the functional modification of the channel proteins, as a consequence of alterations in the redox state of the cell.

Cytoprotective and anti-oxidant genes are up-regulated in denervated muscles

Using RT-PCR analysis, we measured the mRNA abundance of different genes involved in the response to oxidative stress in control and denervated Tibialis Anterior. Data, expressed as percentage expression relative to the housekeeping gene Ckm, are summarized in Figure 4. In 15 day-denervated muscle, a dramatic increase of expression was observed in most examined genes. Most of the genes remained significantly upregulated at 3 months post-denervation compared to control, although their upregulation progressively decreased with denervation time. The decrease in mRNA abundance observed in 3-month

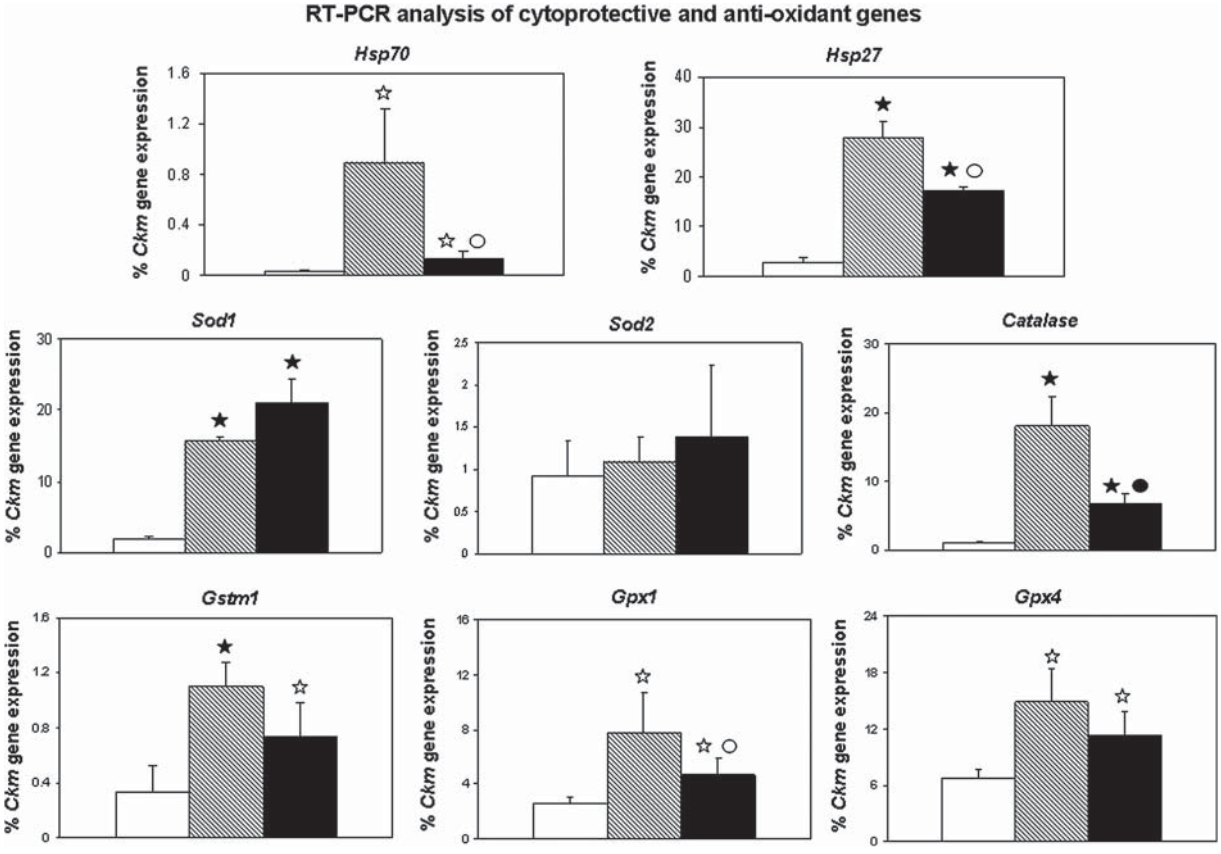

Figure 4. RT-PCR analysis of cytoprotective and anti-oxidant genes. Specific abundance of mRNAs were evaluated in normal control (open bars) or in 15-day denervated (hatched bars) or in 3-month denervated (black bars) rat Tibialis Anterior and was expressed as a percentage of the abundance of the housekeeping gene Muscle creatine kinase (Ckm). Hsp70, Heat shock protein 70; Hsp27, Heat shock protein 27; Sod1, cytoplasmic Cu,Zn-Superoxide dismutase 1, Sod2, mitochondrial Mn-Superoxide dismutase 2; Catalase, Gstm1, Glutathione S-Transferase MU 1; Gpx1, Glutathione Peroxidase 1; Gpx4, Glutathione Peroxidase 4. At least two independent evaluations per sample, each in quadruplicate, were carried out, then data were averaged and are expressed as mean ± SD. ANOVA test analysis was performed. White star: $0.05 \geq p \leq 0.01$ vs control; black star: $p \leq 0.01$ vs control. White ball $0.05 \geq p \leq 0.01$ vs 15-day denervated; black ball: $p \leq 0.01$ vs 15-day denervated.

denervated muscle was in some instance significant with respect to 15-day denervation time and likely reflects the progressive loss of the cell ability to cope with an increasing oxidative stress.

HSP70 and HSP27 are two important heat shock proteins, often involved in the anti-oxidant response. Hsp70 mRNA was expressed at very low levels in control muscle, but increased dramatically upon denervation (32.7- and 4.9-fold at 15 days and 3 months post denervation, respectively). In contrast with Hsp70 mRNA, Hsp27 mRNA was expressed also in control intact TA; however, denervation greatly upregulated its expression (9.6- and 5.9-fold, respectively).

Cytosolic (Cu,Zn-SOD, SOD1) and mitochondrial (Mn-SOD, SOD2) superoxide dismutase are important anti-oxidant enzymes that may be upregulated by oxidative stress. Cu,Zn-Sod mRNA was up-regulated in 15-day denervated muscle (8.5-fold) compared to control; its expression was further enhanced 3 month post-denervation (11.5-fold). On the other hand, the amount of Mn-Sod mRNA was unchanged in denervated TA with respect to control values. Noteworthy, these data are in accordance with SOD1 and SOD2 enzymatic activity (see below).

While SOD enzymes catalyse the dismutation of superoxide anion to hydrogen peroxide, another enzyme (Catalase) is required for hydrogen peroxide detoxification; thus it is not surprising that also Catalase mRNA was found to be up-regulated upon denervation (16.2- and 6.0-fold increase in 15-day and 3-month denervated muscle, respectively).

Messenger RNA abundance of three enzymes involved in the glutathione cycle, namely *Glutathione S-Transferase MU 1* (Gstm1), *Glutathione Peroxidase 1* (Gpx1) and *Glutathione Peroxidase 4* (Gpx4) was similarly increased in denervated TA. Notably, the primers for Gpx4 mRNA were designed in the 3′ region, which is common to all Gpx4 enzymes, independently of their final localization. Figure 4 shows that Gstm1 gene expression was upregulated 3.3- and 2.2-times, Gpx1 mRNA was increased 3.0- and 1.8-fold and Gpx4 mRNA was increased 2.2- and 1.7-fold, in 15-day and 3-month denervated muscle, respectively, with reference to control values.

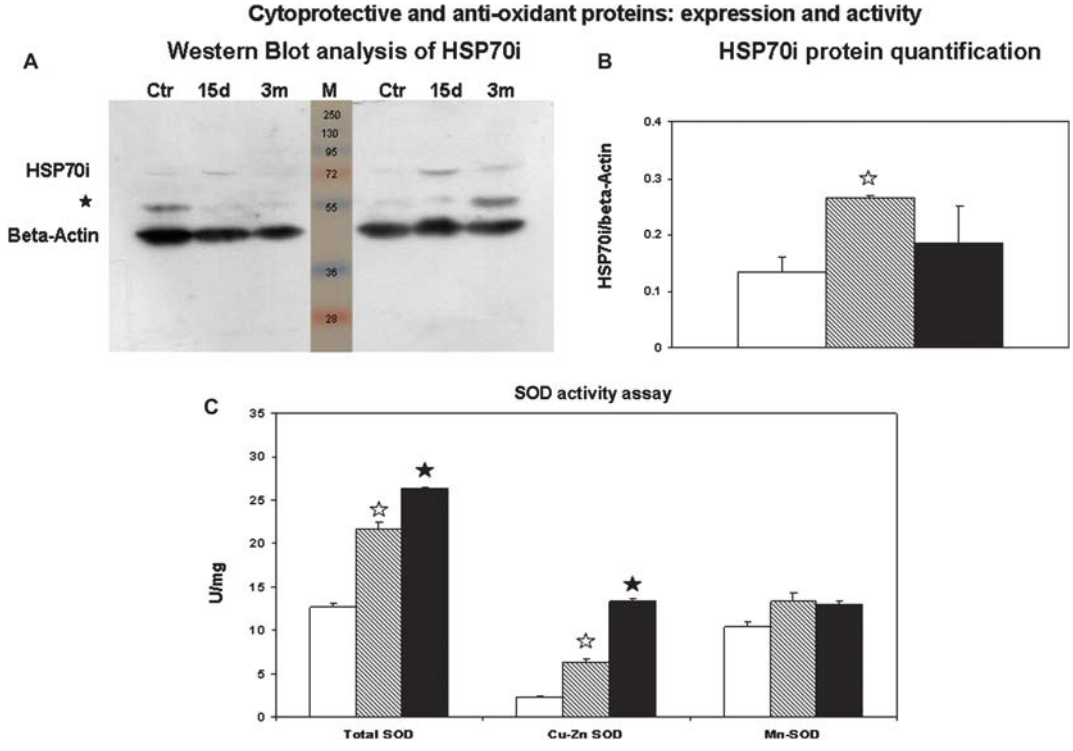

Figure 5. Cytoprotective and anti-oxidant proteins: expression and activity. (A) A representative Western Blot analysis of HSP70i (Mw 70 kDa) in normal control or in 15-day denervated or in 3-month denervated rat Tibialis Anterior. Cytoplasmic beta-Actin (Mw 42 kDa) was evaluated as equal loading control. M, PageRuler™ Plus Prestained Protein Ladder. STAR, aspecific band stained with anti-HSP70 antibody. (B) HSP70i protein quantification. The HSP70i and the beta-Actin WB spots of multiple runs were quantified and HSP70i-to-beta-Actin ratios were calculated and averaged. Results are expressed as mean ± SD. ANOVA test analysis was performed. White star: $0.05 \geq p \leq 0.01$ vs control. Open bars: normal control; hatched bars: 15-day denervated; black bars: 3-month denervated rat Tibialis Anterior. (C) SOD activity assay. SOD enzymatic activity was evaluated as ability to inhibit the $O_2^{\cdot-}$-catalysed formazan dye generation by WST-1 and was expressed in units per milligram protein. The assay was performed in the absence or in the presence of 1 mM KCN, to inhibit the cytoplasmic Cu,Zn-SOD (SOD1). SOD1 was calculated as the difference between total and SOD2 activities. Data from two assays, run in triplicate, were averaged and are expressed as mean ± SD. Open bars: normal control; hatched bars: 15-day denervated; black bars: 3-month denervated rat Tibialis Anterior. ANOVA test analysis was performed. White star: $0.05 \geq p \leq 0.01$ vs control; black star: $p \leq 0.01$ vs control.

HSP70i protein increases following denervation

WB was used in order to evaluate whether the increase in Hsp70 mRNA corresponded to an increase in HSP70i protein in denervated muscle. Figure 5A shows a representative blot, where cytoplasmic actin was used as equal loading control. HSP70i/beta-Actin OD ratio significantly increased 2-fold in 15-day denervated muscle (see Figure 5B), in agreement with the mRNA increase shown in Figure 4.

SOD activity increases following denervation

To evaluate whether the mRNA expression of *Sod1* and *Sod2* was in agreement with the activity of the respective enzymes, the enzymatic activity was assessed in control and denervated TA. As shown in Figure 5C, denervation induced a significant increase of total SOD activity both in 15 day- and 3 month-denervated muscles, as compared to control muscles ($p < 0.05$). Variations in total SOD activity probably result from Cu,Zn-SOD (SOD1), since Figure 5C shows an increase in Cu,Zn-SOD and no variation in Mn-SOD (SOD2) activity at 15 days and 3 months post-denervation. Noteworthy, Cu,Zn-SOD and Mn-SOD enzymatic activity followed the same pattern as mRNA expression (Figure 4).

The above-reported data show that denervated muscle cells react to the increased ROS production by upregulating the synthesis of mRNAs encoding cytoprotective and anti-oxidant enzymes (Figure 4) and of some of their cognate proteins/enzymatic activities (Figure 5). This likely allows for the relatively moderate increase of cellular ROS in the initial phase of the disease. However, the sustained ROS production appears to reduce with time the ability of muscle cells to cope with the increased oxidative stress, thus leading to a weaker cytoprotective response, although some anti-oxidant activity appears to be maintained or even increased in 3-month denervated fibres (see Figure 5C). Notwithstanding the cell's anti-oxidant response, ROS production appears to increase with time (see Figure 1).

Xanthine oxidase and NADPH oxidase do not seem to be involved in the production of ROS in denervated tibialis anterior

Using RT-PCR analysis, we measured the mRNA abundance of Xanthine Dehydrogenase and NADPH Oxidase 1, a potential source of cellular ROS production in the denervated muscle. Data, expressed as percentage expression relative to the housekeeping gene Ckm, are shown in Figure 6A.

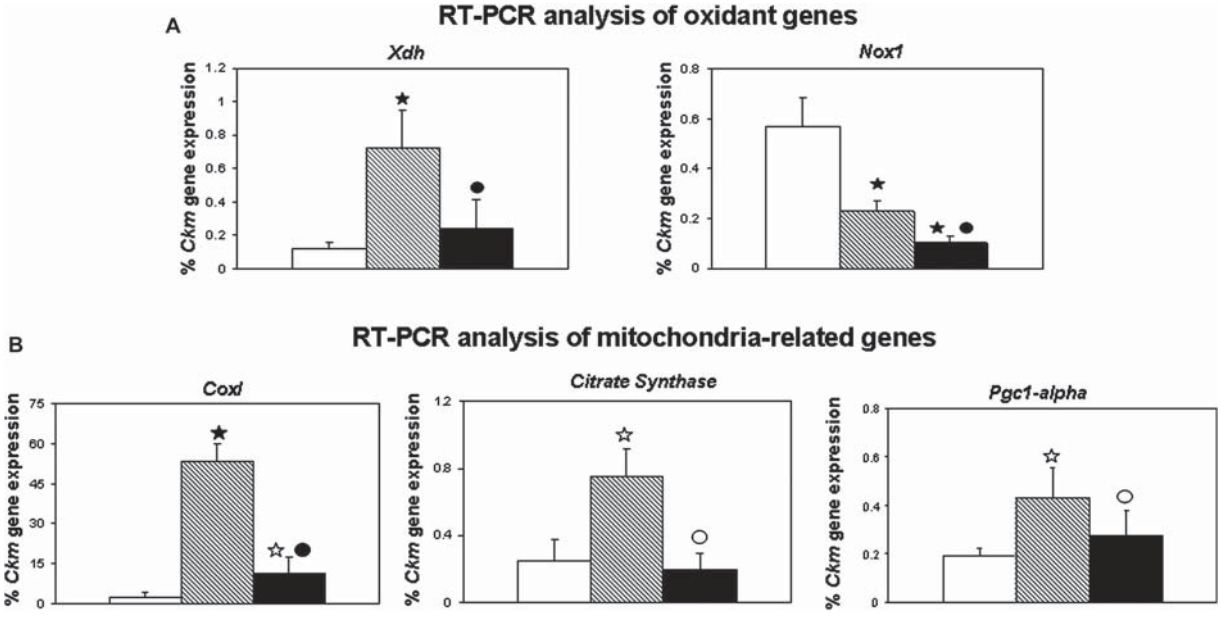

Figure 6. (A) RT-PCR analysis of oxidant genes. Specific abundance of mRNAs was evaluated in normal control (open bars) or in 15-day denervated (hatched bars) or in 3-month denervated (black bars) rat Tibialis Anterior and was expressed as a percentage of the abundance of the housekeeping gene Muscle Creatine Kinase (Ckm). Xdh, Xanthine Dehydrogenase; Nox1, NADPH Oxidase 1. At least two independent evaluations per sample, each in quadruplicate, were carried out, then data were averaged and are expressed as mean ± SD. ANOVA test analysis was performed. Black star: $p \leq 0.01$ vs control. Black ball: $p \leq 0.01$ vs 15-day denervated. (B) RT-PCR analysis of mitochondria-related genes. Specific abundance of mRNAs was evaluated in normal control (open bars) or in 15-day denervated (hatched bars) or in 3-month denervated (black bars) rat Tibialis Anterior and was expressed as a percentage of the abundance of the housekeeping gene Muscle Creatine Kinase (Ckm). CoxI, Cytochrome C Oxidase sub-unit I; Pgc1-α, Peroxisome Proliferator-Activated Receptor gamma, Coactivator-1 alpha. At least two independent evaluations per sample, each in quadruplicate, were carried out, then data were averaged and are expressed as mean ± SD. ANOVA test analysis was performed. White star: $0.05 \geq p \leq 0.01$ vs control; black star: $p \leq 0.01$ vs control. White ball $0.05 \geq p \leq 0.01$ vs 15-day denervated; black ball: $p \leq 0.01$ vs 15-day denervated.

In particular, Xanthine Dehydrogenease (XDH) is a cytoplasmic enzyme that, in the presence of an oxidative environment and of excessive amount of substrates, converts to Xanthine Oxidase, thus producing superoxide anion and hydrogen peroxide. In turn, nucleic acid degradation owing to degenerative processes may lead to excessive amounts of its substrates xanthine and hypoxanthine. We found Xdh mRNA to be upregulated in both 15-day and 3-month denervated muscle (5.8- and 1.9-fold variation with respect to control). This prompted us to examine whether an excess of xantine and/or hypoxanthine was present in denervated muscles, which could account for a Xanthine Oxidase-driven production of ROS. The evaluation was carried out by HPLC; no significant difference among samples was found in both xantine and hypoxanthine concentration (data not shown), thus suggesting that ROS production was not due to Xanthine Oxidase activity in denervated muscles.

NADPH Oxidase 1 (NOX1) is a member of a small family of plasma membrane-associated enzymes that catalyse the production of superoxide by the one-electron reduction of oxygen, using NADPH as the electron donor. We evaluated the abundance of its mRNA and found it to be actually down-regulated in denervated muscles, its amount being 0.4- and 0.2-times that of control muscle in the two time points considered, thus suggesting that a contribution of NADPH Oxidase 1 to the endogenous ROS formation in the denervated muscle is unlikely.

Some mitochondria-related genes are upregulated following denervation

We turned next to examine mitochondria as a potential endogenous source of ROS. Previous observations [33] suggested that ROS induce transcription of factors such as PGC-1alpha that enhance the biogenesis of the oxidative phosphorylation enzymes, notably those encoded by the nuclear genome. By RT-PCR we examined the mRNA abundance of two mitochondrial enzymes, Cytochrome Oxidase sub-unit I (COXI) and Citrate Synthase, encoded by the mitochondrial and the nuclear genome, respectively, and of PGC-1alpha. CoxI mRNA (Figure 6B) resulted significantly up-regulated in 15-day and 3-month post-denervation muscles (21.0- and 4.6-

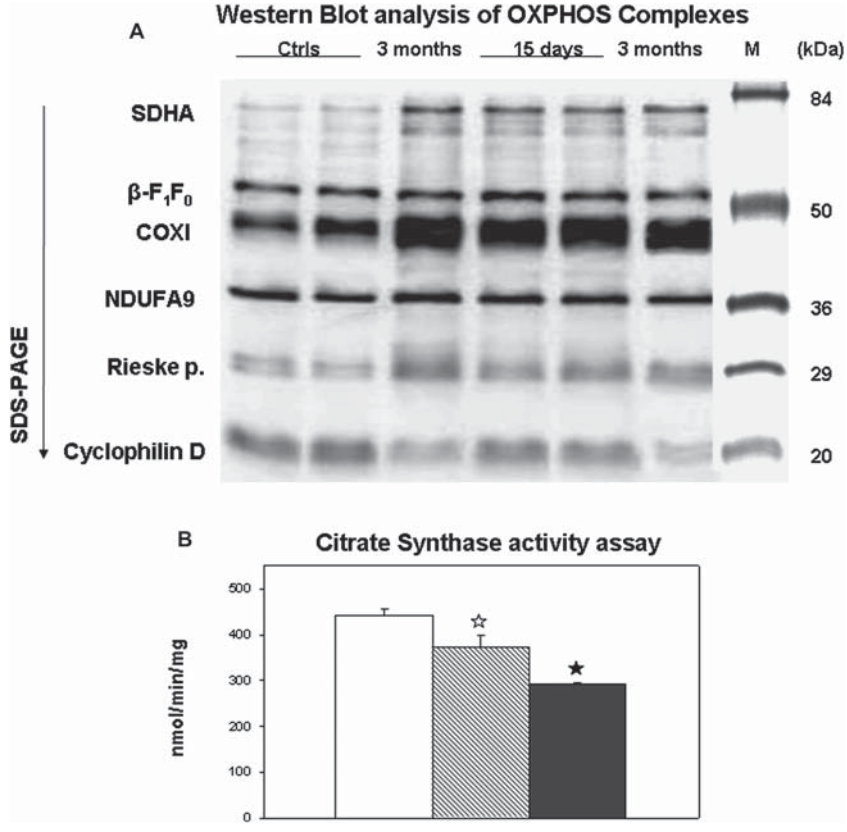

Figure 7. (A) Western Blot analysis of OXPHOS complexes in normal control or in 15-day denervated or in 3-month denervated rat Tibialis Anterior. A representative run out of two for each sample is shown. Proteins analysed here were: NDUFA9 (39 kDa) of Complex I, SDHA (70 kDa) of Complex II, Rieske protein (22 kDa, apparent molecular weight is 30 kDa) of Complex III, COXI (57 kDa, apparent 45 kDa) of Complex IV, β-sub-unit (52 kDa) of the F_1F_0-ATPase, Cyclophilin D (18 kDa), used as an index of mitochondrial mass. M, PageRuler™ Plus Prestained Protein Ladder. (B) Citrate Synthase activity assay. Citrate Synthase enzymatic activity (nmol/min/mg of protein) was evaluated by measuring the rate of free coenzyme A release. Data from two independent assays were averaged and are expressed as mean ± SD. Open bars: normal control; hatched bars: 15-day denervated ; black bars: 3-month denervated rat Tibialis Anterior. ANOVA test analysis was performed. White star: $0.05 \geq p \leq 0.01$ vs control; black star: $p \leq 0.01$ vs control.

times, respectively) compared to control. Citrate Synthase mRNA expression (Figure 6B) was found to be increased when examined 15 days following denervation (3.0-fold increase), but returned to control levels following 3-month denervation. Notably, PGC-1 alpha mRNA followed the same pattern of expression as the mRNA coding for Citrate Synthase (Figure 6B). In fact, it was found to be increased by a factor of 2.2 in 15-day denervated muscles, but returned to control levels following 3-month denervation.

Mitochondrial complex protein expression is unbalanced in denervated muscles

The expression of some mitochondrial enzymes involved in oxidative phosphorylation was analysed by Western Blot. Impairment or differential protein expression in mitochondrial electron transport chain elements might lead to an increase in ROS production. As shown in Figure 7, we found that COXI (Cytochrome Oxidase sub-unit I), a member of Complex IV, was dramatically up-regulated in 15 day and 3-month denervated muscle compared to control. Noteworthy, these data are in accordance with those obtained for COXI mRNA abundance. Also Rieske protein and Succinate Dehydrogenase Complex sub-unit A (SDHA) (belonging to Complex III and II, respectively) were increased, although to a milder extent, in denervated muscle. A slight increase was also observed in the β sub-unit of the -F_1F_0 ATP Synthase complex and NDUFA9 (NADH Dehydrogenase (ubiquinone) 1alpha sub-complex 9), a protein belonging to Complex I. Cyclophilin D was used as a marker of the mitochondrial mass; notably, it displayed a substantial decrease in 3-month denervated muscle.

Citrate Synthase activity, another widely accepted marker of mitochondrial mass, was evaluated as well (Figure 7B); data showed a small but significant decrease (–15.0%; $p < 0.05$) in 15-day denervated muscle and a further decrease (–34.0%; $p < 0.01$) in 3-month denervated muscle. It should be noted that these data were not in agreement with the mRNA expression data (Figure 6B); at present, there is no explanation for this result, although oxidative stress may lead to one or all the following outcomes: partial inactivation of the protein, enhanced protein degradation or lack of mRNA translation.

Although other sources of ROS cannot be excluded, data presented in Figure 7 suggest that the enhanced ROS production following denervation is likely to originate mostly from the unbalance of expression of the different complexes of the mitochondrial respiratory chain. Indeed all these enzymes are overexpressed in denervated muscle, as shown both at the transcription level (Figure 6B) and in the translated protein sub-units (Figure 7A); compared to COXI, Complex I and ATP Synthase appear to be increased only slightly, perhaps as a result of their enhanced protein degradation, since Complex I and ATP Synthase sub-units appear to be more susceptible to oxidative damage with respect to COXI [34,35]. Such unbalance may represent a condition favouring the increase of ROS production [36,37]; in particular Complex I becomes an important source of ROS when electron transfer from NADH to ubiquinone is impaired [38]; moreover Complex I is particularly susceptible to ROS damage [39], thus easily establishing a vicious circle of enhanced ROS generation.

Mitochondria thus appear to be the major source of the increased ROS production in denervated muscle; in this view, it may be surprising that we observe an increase in the activity of the cytosolic form of SOD rather than of the mitochondrial one. Other authors have assessed the protein amount of Mn-SOD in the mitocondria of denervated muscles and they found it to be decreased [40,41]. Thus, our results appear to suggest that the mitochondria are not only the primary source of the increased ROS production, but also confirm that they are unable to quench such an increase by using their internal defences. On the other hand, the whole cell appears to lose with time the ability to quench the overall ROS production, as suggested by the decrease in Catalase and GPX1 mRNA synthesis.

Calcium-activated phospholipase 2a mRNA is upregulated in denervated muscles

A recent work [42] reported an increase in fatty acid hydroperoxides in surgically denervated rat skeletal muscles, examined 7 days post-denervation, and proposed the activation of cytosolic phospholipase A2 as a potential source of these hydroperoxides. The phospholipase cPLA2α is a calcium-activated cytosolic enzyme that associates with cell membranes and causes the release of fatty acid hydroperoxides, with a preference for arachidonic acid. We measured cPLA2α mRNA abundance and found (Figure 8) that it was upregulated in 15-day denervated muscle (7.2-fold variation with respect to control); the increase was lesser (1.7-fold) in 3-month denervated muscle. However, since cPLA2α is a calcium-dependent cytosolic enzyme, the increase in its expression may be ineffective if not accompanied by an increase in $[Ca^{2+}]_i$. As shown in Figure 3, we found both sarcolemmal and SR Ca^{2+} pumps to be partially inactivated in denervated muscles; the impairment in Ca^{2+}export is expected to lead to an increase in its cytosolic concentration. Further independent data [43] suggest that $[Ca^{2+}]_i$ may be increased up to 150-fold upon denervation. Thus, the early increase in cPLA2α mRNA (shown here) and protein [42] abundance is likely to result in a significant increase in fatty acid hydroperoxide concentration. Although cPLA2α increase may not be sustained in longer-standing denervated TA, $[Ca^{2+}]_i$ is nevertheless elevated and may support its activation. Lipid hydroperoxides are detoxified by the

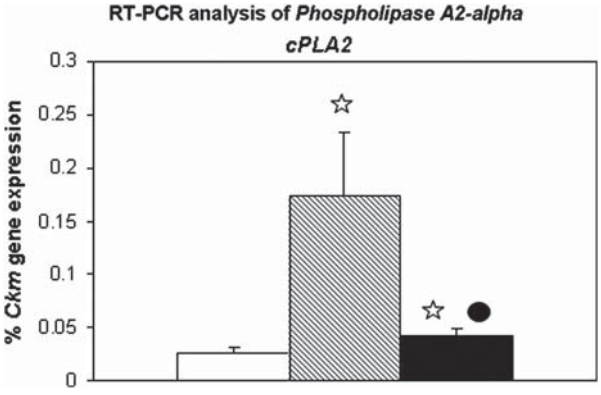

Figure 8. RT-PCR analysis of Phospholipase A2-alpha. Specific abundance of cPLA2α—Calcium-dependent cytosolic Phospholipase A2-alpha—mRNA was evaluated in normal control (open bars) or in 15-day denervated (hatched bars) or in 3-month denervated (black bars) rat Tibialis Anterior and was expressed as a percentage of the abundance of the housekeeping gene Muscle Creatine Kinase (Ckm). At least two independent evaluations per sample, each in quadruplicate, were carried out, then data were averaged and are expressed as mean ± SD. ANOVA test analysis was performed. White star: $0.05 \geq p \leq 0.01$ vs control; black ball: $p \leq 0.01$ vs 15-day denervated.

seleno-enzyme Gpx4 [44] which is associated with membranes, including the mitochondrial membranes. Its over-expression was found to protect rabbit aortic smooth muscle cells from apoptosis [45]. We actually observed an increase in GPX4 mRNA expression in the denervated muscle cells (Figure 4), a finding that supports the hypothesis that the muscle fibres try to cope with an increase in lipid hydroperoxides.

In our view, the increased ROS production, occurring in mitochondria as a consequence of the unbalance in some respiratory enzymes, may lead to the peroxidation of mitochondrial membranes. Then, in a calcium-enriched cytoplasm, the increased activity and the increased expression [42] of calcium-activated phospholipase A2 may lead to the release of lipid hydroperoxides, which may not be counterbalanced by an adequate increase in Gpx4 activity.

In the initial response to denervation (i.e. at the 15-day time point), muscle cells are apparently rather able to react to the increased ROS production, by upregulating their cytoprotective and anti-oxidant proteins; transcriptional mechanisms leading to the upregulation of mitochondrial enzymes are also activated (see Figure 6B); however, possibly owing to oxidative damage, some of the induced proteins may become inactive or may be degraded; thus, the ROS-induced upregulation of some OXPHOS enzymes (via PGC1-α) may lead to a further unbalance of the enzymes involved in the respiratory chain and to an increase in ROS production, somehow accompanied by a reduced ability to detoxify excess ROS. The effect of denervation on mitochondrial biogenesis appears to contrast the effect of unloading that also leads to atrophy, but with a shift from aerobic to glycolytic metabolism [46].

Conclusion

As mentioned above, it has been already shown that a number of conditions leading to muscle atrophy are associated to an increased mitochondrial ROS production [6]; the relevant new data presented here identify the cause of such increase in an unbalance in the relative amount of some components of the mitochondrial respiratory chain. The present study adds also more information on the cellular defence responses and shows that they *decrease* with denervation time, concomitantly with an increase in ROS production and in oxidative stress-induced damage. In fact, massive degenerative processes progressively take place in the denervated muscle cells, as far as gross morphology, ultrastructural organization and functional responses are concerned [10,47,48]. Such progressive degeneration may be accelerated or even prompted by the oxidative stress occurring upon denervation, as shown in the present paper. This suggests that an anti-oxidant therapeutical strategy [49,50] might be advisable in a wide spectrum of diseases and conditions where the nerve-muscle connection is impaired. On the other hand, even after long-term denervation, atrophic and damaged muscle cells are still actively attempting to regenerate [24]; this shows that there is lasting ground for improvement and healing provided that endogenous sources of injury (i.e. ROS), are removed.

Acknowledgements

The Perkin-Elmer 5700 Real Time PCR Apparatus we used had been donated by the *Fondazione Cassa di Risparmio di Bologna*.

Declaration of interest: The present work was financially supported by Italian MIUR funds to the Department of Histology, Embryology, and Applied Biology, to the Department of Biochemistry, Bologna University, Italy, and to the Laboratory of Translational Myology, Padua University, Italy; Italian C.N.R. funds to the Institute of Neuroscience, University of Padova, Italy; Austrian National Cofinancing by the Ministry of Science(BM:BWK); European Regional Development Fund (ERDF, Interreg IIIa). The authors report no conflicts of interest. The authors alone are responsible for the content and writing of the paper.

References

[1] Tisdale MJ. Cancer cachexia: metabolic alterations and clinical manifestations. Nutrition 1997;13:1–7.
[2] Monani UR. Spinal muscular atrophy: a deficiency in a ubiquitous protein; a motor neuron-specific disease. Neuron 2005;48:885–896.
[3] Porter MM, Vandervoort AA, Lexell J. Aging of human muscle: structure, function and adaptability. Scand J Med Sci Sports 1995;5:129–142.

[4] Fulle S, Protasi F, Di Tano G, Pietrangelo T, Beltramin A, Boncompagni S, Vecchiet L, Fanó G. The contribution of reactive oxygen species to sarcopenia and muscle ageing. Exp Gerontol 2004;39:17–24.

[5] Muller FL, Song W, Liu Y, Chaudburi A, Picke-Dahl S, Strong R, Huang T-T, Epstein CJ, Robert LJ 2nd, Cscte M, Faulkner JA, Van Remmen H. Absence of CuZn superoxide dismutase leads to elevated oxidative stress and acceleration of age-dependent skeletal muscle atrophy. Free Radic Biol Med 2006; 40:1993–2004.

[6] Muller FL, Song W, Jang YC, Liu Y, Sabia M, Richardson A, Van Remmen H. Denervation-induced skeletal muscle atrophy is associeted with increased mitochondrail ROS production. Am J Physiol Regul Integr Comp Physiol 2007;293: R1159–R1168.

[7] Debrowolny G, Aucello M, Rizzuto E, Beccafico S, Mammucari C, Boncompagni S, Belia S, Wannenes F, Nicoletti C, Del Prete Z, Rosenthal N, Molinaro M, Protasi F, Fanó G, Sandri M, Musarò A. Skeletal muscle is a primary target of SOD-1 ^{G93A}-mediated toxiticy. Cell Metab 2008;8:425–436.

[8] McCord JM. Oxygen-derived free radicals in postischemic tissue injury. N Engl J Med 1985;312:159–163.

[9] Kostrominova TY, Dow DE, Dennis RG, Miller RA, Faulkner JA. Comparison of gene expression of 2-mo denervated, 2-mo stimulated-denervated, and control rat skeletal muscles. Physiol Genomics 2005;22:227–243.

[10] Kern H, Boncompagni S, Rossini K, Mayr W, Fanó G, Zanin ME, Podhorska-Okolow M, Protasi F, Carraro U. Long-term denervation in humans causes degeneration of both contractile and excitation-contraction coupling apparatus, which is reversible by Functional Electrical Stimulation (FES): a role for myofiber regeneration? J Neuropathol Exp Neurol 2004; 63:919–931.

[11] Carlson BM, Borisov AB, Dedkov EI, Khalyfa A, Kostrominova TY, Macpherson PCD, Wang E, Faulkner JA. Effects of long-term denervation on skeletal muscle in old rat. J Gerentol 2002;57A:B366–B374.

[12] Sun J, Xu L, Eu JP, Stamler JS, Meissner G. Classes of thiols that influence the activity of the skeletal muscle calcium release channel. J Biol Chem 2001;276:15625–15630.

[13] Kandarian SC, Jackman RW. Intracellular signaling during skeletal muscle atrophy. Muscle Nerve 2006;33:155–165.

[14] Li YP, ChenY, John J, Moylan J, Jin B, Mann DL, Reid MB. TNF-α acts via p38 MAPK to stimulate expression of the ubiquitin ligase atrogin1/MAFbx in skeletal muscle. FASEB J. 2005;19:362–370.

[15] Sandri M. Signaling in muscle atrophy and hypertrophy. Physiology 2008;23:160–170.

[16] Degli Esposti M. Measuring mitochondrial reactive oxygen species. Methods 2002;26:335–340.

[17] Cathcart R, Schwiers E, Ames BN. Detection of picomole levels of hydroperoxides using a fluorescent dichlorofluorescein assay. Anal Biochem 1983;134:111–116.

[18] Rock E, Mammar MS, Vignon X, Thomas MA, Viret J. Abnormal fluidity state in membranes of malignant hyperthermia pig skeletal muscle. Arch Biochem Biophys 1990; 281:36–40.

[19] Renganathan M, Messi ML, Delbono O. Dihydropyridine receptor-ryanodine receptor uncoupling in aged skeletal muscle. J Membr Biol 1997;157:247–253.

[20] Mecocci P, Fanó G, Fulle S, MacGarvey U, Shinobu L, Polidori MC, Cherubini A, Vecchiet J, Senin U, Beal MF. Age-dependent increases in oxidative damage to DNA, lipids, and proteins in human skeletal muscle. Free Radic Biol Med 1999;26:303–308.

[21] Fulle S, Belia S, Vecchiet J, Morabito C, Vecchiet L, Fanò G. Modification of the functional capacity of sarcoplasmic reticulum membranes in patients suffering from chronic fatigue syndrome. Neuromuscul Disord 2003;13:479–484.

[22] Chomczynski P, Sacchi N. Single-step method of RNA isolation by acid guanidinium thiocyanate-phenol-chloroform extraction. Anal Biochem 1987;162:156–159.

[23] Marini M, Lapalombella R, Margonato V, Ronchi R, Samaja M, Scapin C, Gorza L, Maraldi T, Carinci P, Ventura C, Veicsteinas A. Mild exercise training, cardioprotection and stress genes profile. Eur J Appl Physiol 2007;99:503–510.

[24] Lapalombella R, Kern H, Adami N, Biral D, Zampieri S, Scordari A, di Tullio S, Marini M. Persistence of regenerative myogenesis in spite of down-regulation of activity-dependent genes in long-term denervated rat muscle. Neurol Res 2008;30:197–206.

[25] Adams L, Carlson BM, Henderson L, Goldman D. Adaptation of nicotinic acetylcholine receptor, myogenin, and MRF4 gene expression to long-term muscle denervation. J Cell Biol 1995;131:1341–1349.

[26] Dedkov AI, Kostrominova TY, Borisov AB, Carlson BM. Reparative myogenesis in long-term denervated skeletal muscle of adult rats results in a reductionof the satellite population. Anat Rec 2001;263:139–154.

[27] Livak JK, Schimitten TD. Analysis of relative gene expression data using real-time quantitative PCR and the $2^{-\Delta\Delta CT}$ method. Methods 2001;25:402–408.

[28] Peskin AV, Winterbourn CC. A microtiter plate assay for superoxide dismutase using a water-soluble tetrazolium salt (WST-1). Clin Chim Acta 2000;293:157–166.

[29] Zhou JY, Prognon P. Raw material enzymatic activity determination: a specific case for validation and comparison of analytical methods. The example of superoxide dismutase (SOD). J Pharm Biomed Anal 2006;40:1143–1148.

[30] Baracca A, Sgarbi G, Mattiazzi M, Casalena G, Pagnotta E, Valentino ML, Moggio M, Lenaz G, Carelli V, Solaini G. Biochemical phenotypes associated with the mitochondrial ATP6 gene mutations at nt8993. Biochim Biophys Acta 2007;1767:913–919.

[31] Lowry OH, Rosebrough NJ, Farr AL, Randall RJ. Protein measurement with the Folin phenol reagent. J Biol Chem 1951;193:265–275.

[32] Genova ML, Baracca A, Biondi A, Casalena G, Faccioli M, Falasca AI, Formiggini G, Sgarbi G, Solaini G, Lenaz G. Is supercomplex organization of the respiratory chain required for optimal electron transfer activity? Biochim Biophys Acta 2008;1777:740–746.

[33] Spiegelman BM. Transcriptional control of mitochondrial energy metabolism through the PGC1 coactivators. Novartis Found Symp 2007;287:60–63; discussion 63–69.

[34] Guerrieri F, Vendemiale G, Grattagliano I, Cocco T, Pellecchia G, Altomare E. Mitochondrial oxidative alterations following partial hepatectomy. Free Radic Biol Med 1999; 26:34–41.

[35] Fato R, Bergamini C, Leoni S, Strocchi P, Lenaz G. Generation of reactive oxygen species by mitochondrial complex I: implications in neurodegeneration. Neurochem Res 2008;33: 2487–2501.

[36] Lenaz G. The mitochondrial production of reactive oxygen species: mechanisms and implications in human pathology. IUBMB Life 2001;52:159–164.

[37] Jezek P, Hlavatá L. Mitochondria in homeostasis of reactive oxygen species in cell, tissues, and organism. Int J Biochem Cell Biol 2005;37:2478–2503.

[38] Fato R, Bergamini C, Bortolus M, Maniero AL, Leoni S, Ohnishi T, Lenaz G. Differential effects of mitochondrial Complex I inhibitors on production of reactive oxygen species. Biochim Biophys Acta 2009;1787:384–392.

[39] Paradies G, Petrosillo G, Pistolese M, Di Venosa N, Federici A, Ruggiero FM. Decrease in mitochondrial complex I activity in ischemic/reperfused rat heart: involvement of reactive oxygen species and cardiolipin. Circ Res 2004; 94:53–59.

[40] Siu PM, Always SE. Mitochondria-associated apoptotic signaling in denervated rat skeletal muscle. J Physiol 2005; 565:309–323.
[41] Adhihetty PJ, O'Leary MFN, Chabi B, Wicks KL, Hood DA. Effect of denervationon mitochondrially mediated apoptosis in skeletal muscle. J Appl Physiol 2007;102:1143–1151.
[42] Bhattacharya A, Muller FL, Liu Y, Sabia M, Liang H, Song W, Jang YC, Ran Q, Van Remmen H. Denervation induces cytosolic phospholipase A2-mediated fatty acid hydroperoxide generation by muscle mitochondria. J Biol Chem 2009;284: 46–55.
[43] Squecco R, Carraro U, Kern H, Pond A, Adami N, Biral D, Vindigni V, Boncompagni S, Pietrangelo T, Bosco G, Fanò G, Marini M, Abruzzo PM, Germinario E, Danieli-Betto D, Protasi F, Francini F, Zampieri S. A sub-population of rat muscle fibers maintains an assessable excitation-contraction coupling mechanism after long-standing deneravtion, despite lost contractility. J Neuropathol Exp Neurol 2009;68:1256–1268.
[44] Toppo S, Flohé L, Ursini F, Vanini S, Maiorino M. Catalytic mechanisms and specificities of glutathione peroxidases: variations of a basic scheme. Biochim Biophys Acta 2009;1790: 1486–1500.
[45] Brigelius-Flohé R, Maurer S, Lötzer K, Böl G, Kallionpää H, Lehtolainen P, Viita H, Ylä-Herttuala S. Overexpression of PHGPx inhibits hydroperoxide-induced oxidation, NFkappaB activation and apoptosis and affects oxLDL-mediated proliferation of rabbit aortic smooth muscle cells. Atherosclerosis 2000;152:307–316.
[46] Moriggi M, Cassano P, Vasso M, Capitanio D, Fania C, Musicco C, Pesce V, Gadaleta MN, Gelfi CA. DIGE approach for the assessment of rat soleus muscle changes during unloading: effect of acetyl-L-carnitine supplementation. Proteomics 2008;8:3588–3604.
[47] Boncompagni S, Kern H, Rossini K, Mayr W, Carraro U, Protasi F. Structural differentiation of skeletal muscle fibres in absence of innervation in humans. Proc Natl Acad Sci USA 2007;104:19339–19344.
[48] Kern H, Carraro U. Translational myology focus on clinical challenges of functional electrical stimulation of denervated muscle. Basic Appl Myol/Eur J Translat Myol 2008;18: 37–100.
[49] Kondo H, Miura M, Itokawa Y. Oxidative stress in skeletal muscle atrophied by immobilization. Acta Physiol Scand 1991;142:527–528.
[50] Golding JD, Rigley MacDonald SD, Juurlink BHJ, Rosser BWC. The effect of glutamine on locomotor performance and skeletal muscle myosins following spinal cord injury in rats. J Appl Physiol 2006;101:1045–1052.

This paper was first published online on Early Online on 18 March 2010.